Inactivation Of Encapsulated Cells And Their Therapeutic Effects By Means Of TGL Triple-Fusion Reporter/Biosafety Gene.

Edorta Santos[1,2], Leire Larzabal[3], Alfonso Calvo[3], Gorka Orive[1,2], José Luis Pedraz[1,2], Rosa María Hernández[1,2]

[1]NanoBioCel Group, Laboratory of Pharmaceutics, University of the Basque Country, School of Pharmacy, Vitoria, Spain; [2]Biomedical Research Networking Center in Bioengineering, Biomaterials and Nanomedicine (CIBER-BBN), Vitoria, Spain.
[3]Laboratory of Novel Therapeutic Targets, Centre for Applied Biomedical Research (CIMA), University of Navarra. Avenida Pío XII 57, 31007 Pamplona, Spain.

Correspondence should be addressed to: Rosa María Hernández

(rosa.hernandez@ehu.es)

Laboratory of Pharmacy and Pharmaceutical Technology
Faculty of Pharmacy UPV/EHU
Paseo de la Universidad nº 7
01006 Vitoria-Gasteiz, Spain
Phone: +34-945013095
Fax: +34-945013040

Keywords: microcapsule, TGL, drug delivery, biosafety, HSV-TK

Running title: Inactivation of encapsulated cells

ABSTRACT

The immobilization of cells within alginate-poly-L-lysine-alginate (APA) microcapsules has been demonstrated to be an effective technology design for long term delivery of therapeutic products. Despite promising advances, biosafety aspects still remain to be improved. Here, we describe a complete characterization of the strategy based on TGL triple-fusion reporter gene – which codifies for Herpes Simplex virus type 1 thymidine-kinase (HSV1-TK), green fluorescence protein (GFP) and Firefly Luciferase – ($SFG_{NES}TGL$) to inactivate encapsulated cells and their therapeutic effects. Myoblasts genetically engineered to secrete erythropoietin (EPO) were retroviraly transduced with the $SFG_{NES}TGL$ plasmid to further characterize their ganciclovir (GCV)-mediated inactivation process. GCV sensitivity of encapsulated cells was 100-fold lower when compared to cells plated onto 2D surfaces. However, the number of cells per capsule and EPO secretion decayed to less than 15% at the same time that proliferation was arrested after 14 days of GCV treatment in vitro. In vivo, ten days of GCV treatment was enough to restore the increased hematocrit levels of mice implanted with encapsulated TGL-expressing and EPO-secreting cells. Altogether, these results show that TGL triple-fusion reporter gene may be a good starting point in the search of a suitable biosafety strategy to inactivate encapsulated cells and control their therapeutic effects.

INTRODUCTION

Cell microencapsulation comprises the immunoisolation of non-autologous cells to supply the lack of functional organs or target the sustained delivery of therapeutic factors. Recent studies from the past decade have served to pave the way for leading this biotechnology close to the patient in several clinical trials [1-7]. During this course, many cells and different biomaterials have been assayed in numerous pre-clinical studies in order to find the most balanced and suitable combination [8-11]. Determining the mechanical stability [12,13], biocompatibility [14-16] and long-term functionality issues [17], among others, have been the central focus of past investigations. In addition, great advances have also been made regarding biomaterial functionalization [18], size reduction of the particles [19,20], xenogenic implants [21-23] or even in the nascent understanding of cell behavior within the capsules [24,25]. Nonetheless, many challenges still remain.

Nowadays, the biosafety of these biosystems is clearly one of the prime concerns among the scientist involved in this field. The possibility to inactivate the implant once the therapy reaches its final goal and/or in case of undesirable deleterious effects, represents a necessary requirement for cell microencapsulation. Recently, we proposed TGL triple-fusion reporter gene, which codifies for green fluorescence protein (GFP), Firefly Luciferase and Herpes Simplex virus type 1 thymidine-kinase (HSV1-TK), as a promising alternative for such aim [26]. In a similar fashion, Aebischer's group reported the pre-implantation use of HSV1-TK gene to eliminate the remaining percentage of dividing C_2C_{12} myoblasts encapsulated in hollow fibers and induced to differentiation

[27]. Nevertheless, the efficacy of this reporter/biosafety plasmid to control the therapeutic effects of enclosed cells has not been assessed yet.

GCV-mediated apoptosis has been well described for cells plated onto 2D surfaces, emphasizing its replication dependency and defining in detail the time intervals required for each phase [28,29]. However, due to the remarkably different behavior shown by cells within three-dimensional scaffolds [30], such inactivation process must be re-characterized and described in detail for cells encapsulated within polymeric matrices in order to understand and validate its use within these platforms.

Erythropoietin (EPO), a glycoprotein hormone responsible for erythropoiesis [31], represents an especially attractive molecule to be studied as a candidate model. Given that baseline EPO serum concentration only prompts minimal EPO dose-response at erythrocyte precursor level in the bone marrow, a slight increase in EPO is enough to stimulate erythropoiesis [32]. Furthermore, its expression and bioactivity in vivo can be easily monitored by just following the hematocrit level [33]. Thus, unless an effective elimination of the implant and its therapeutic effect is reached, hematocrit levels of the host will reflect the existence of remaining non-inactivated functional cells in the implant.

This study is aimed to explore the gene suicide properties of the TGL triple-fusion reporter gene as a possible biosafety tool in the progressive adaptation of cell microencapsulation to the clinical practice requirements. Murine C_2C_{12} cell line, genetically engineered to secrete EPO and transduced with the TGL triple-fusion reporter gene, was encapsulated within alginate-poly-L-lysine-alginate (APA)

microcapsules for further investigating GCV-mediated inactivation process. Initial series of in vitro experiments served to compare GCV sensitivity of cells in 2D and 3D, as well as to observe how inactivation process affects cell proliferation, the total number of living cells per capsule and EPO secretion during different time-points. Finally, this strategy was assayed in Balb/c mice to confirm the arrest of the therapeutic effects and the restoring of the physiological function in animals.

MATERIAL AND METHODS

Cell culture

C_2C_{12} myoblasts derived from the skeletal muscle of a C3H mouse and genetically engineered to express the TGL triple-fusion reporter gene, or EPO or both of them were maintained in complete medium, consisting of: Dulbecco's modified Eagle medium (DMEM) supplemented with 10% fetal bovine serum (FBS), L-glutamine to a final concentration of 2 mM, 4.5 g/L glucose and 1% antibiotic/antimycotic solution. Cells were plated in T-flasks, grown at 37ºC in a 5% CO_2/95% atmosphere and passaged every 2-3 days. All reagents were purchased from Gibco BRL (Invitrogen S.A., Spain).

Generation of the different employed clone types

TGL-EPO clone: C_2C_{12} myoblasts genetically engineered to secrete EPO (kindly provided by Dr. Aebischer P) were retroviraly transduced with the $pSFG_{NES}TGL$ plasmid to express TGL, as previously reported by our group [26]. Briefly, the amphopack-293 packaging cell line (Clontech) was transfected with $pSFG_{NES}TGL$ purified retrovector, kindly donated by Dr. Ponomarev (Memorial Sloan Kettering Cancer Centre, NY) [34]. Transfection was performed using Lipofectamine 2000 (Invitrogen, Carlsbad,CA,USA) according to manufacturer´s protocol. 48h after transfection, culture supernatant containing virus from packaging cells and 7.5ug/mL Polybrene (hexadimethrine bromide; Sigma, St Louis, MO, USA) were added in two different 24h cycles to the C_2C_{12} cells. The plasmid $pSFG_{NES}TGL$ is characterized by the presence of green fluorescent protein (GFP), luciferase and thymidine kinase genes

fused together. Vector containing GFP+ cells were selected by fluorescent-activated cell sorting (FACS) (Suppl. Fig. 1).

TGL clone: This clone was obtained following the same procedure carried out for TGL-EPO clone but starting from pure EPO non-secreting C_2C_{12} myoblasts.

EPO clone: This was the name given to EPO-secreting cells non-subjected to transduction with pSFG$_{NES}$TGL vector (Suppl. Fig. 2 shows the EPO secretion of each clone).

Cell microencapsulation

Genetically engineered C_2C_{12} myoblasts were encapsulated into APA microcapsules using an electrostatic droplet generator and following a brief modification of the procedure established by Lim & Sun's [35]. Briefly, cells were harvested from monolayer cultures using trypsin-EDTA (Invitrogen), filtered through a 40 µm pore mesh and resuspended in 1.5% sodium alginate at 5 x 10^6 cells/mL density. The resulted suspension was extruded in a sterile syringe through a 0.25 mm needle at a 5.9 ml/h flow rate using a peristaltic pump. The drops were collected in a 55 mM $CaCl_2$ solution and maintained under agitation for 15 min after the end of the process in order to enable complete gelation of all the beads. Subsequently, these particles were suspended in 0.05% PLL solution for 5 min, washed twice with 10 mL of mannitol 1% and coated again with another layer of 0.1% alginate for 5 min. The whole process was carried out at room temperature and under aseptic conditions. Resulting microcapsules were cultured in complete medium at 37ºC in a 5% CO2/95% air atmosphere standard

incubator and passaged every 2-3 days if assayed in vitro. For the overdose model a cell load of 20 x 10^6 cells/mL was encapsulated varying the optimal conditions of the encapsulation process to produce defective and overloaded microcapsules. Ultra pure low-viscosity high glucuronic acid alginate (UPLVG) was purchased from FMC Biopolymer, Norway. Poly-*L*-lysine (PLL hidrobromide M_w 15 000–30 000 Da) was obtained from Sigma Aldrich (St. Louis, MO, USA).

GCV sensitivity

For 2D GCV sensitivity assay 100 µL of cell suspension (1000 cells/well) were plated onto a 96 well plate, incubated for 12 h and subsequently subjected to increased concentrations of GCV for 7 days. Metabolic activity of encapsulated cells was measured afterwards using CCK-8 cell viability kit (Dojindo): 10 µL of CCK-8 were added to each well and after 4 h incubation at 37ºC, the plate was read at 450 nm to assess colour development. All values were corrected with the reference wavelength at 690 nm and normalized against the mean value of 3 blank wells (medium). For sensitivity assays carried out with encapsulated cells, same procedure was repeated by placing 7000 cells/well (≈ 60 caps/well). Results are expressed as the mean of 7 independent samples ±S.D per assayed condition and study group.

Quantification of the total number of living cells per capsule

In order to determine the exact number of living cells, enclosed cells were firstly de-encapsulated using 500 µg/mL of alginate lyase (Sigma-Aldrich) and filtered through a 40 µm mesh filter. LIVE/DEAD kit (Invitrogen) was used to differentiate living and

dead cells, by adding 20 µL of calcein (50 µM) and 4 µL of ethidium homodimer (200 µM) to each milliliter of cell suspension. After incubation of samples for 20 min at room temperature and protected from light, cells were counted by means of flow cytometry (BD FACSCalibur) using Trucount Tubes (BD). Before the assessment, both positive (living cells harvested from 2D monolayer) and negative (dead cells treated with ethanol) controls were dyed with LIVE/DEAD kit and run in Trucount Tubes in order to set flow cytometry parameters. Cells positively stained with calcein (living cells) were detected in the FL1 channel (green fluorescence). Cells stained with ethidium homodimer were detected in the FL3 channel (red fluorescence). FL2 channel (orange fluorescence) was employed for the capture of Trucount Tubes beads. Living cells are shown as green dots in the FL1/FL3 dot plot within UP LEFT quadrant (healthy cells) and UP RIGHT quadrant (damaged but still living cells), whereas dead cells appear as red dots in the DOWN LEFT quadrant. Number of living cells per capsule was calculated on the basis of a known number of microcapsules in a particular volume. All GCV exposure times were assayed in triplicate for both groups, and obtained values are shown as the mean +S.D.

Cell viability

Encapsulated cells were dyed with the LIVE/DEAD kit (Invitrogen) following manufacturer's indications and after 30 min, fluorescence micrographs were taken with an epi-fluorescence microscope (Nikon TSM).

Measurement of EPO secretion

Cell supernatants were assayed for EPO secretion using the Quantikine IVD Human Erythropoietin ELISA Kit purchased from R&D Systems (Minneapolis, MN). Standards and samples were run in duplicate according to the procedure specified in the kit. The EPO secretion of 100 µL capsules (single dose)/mL (the equivalent of 5 x 10^5 cells/mL) was measured for a 24 h release period in triplicate per study group. Results are expressed as mean + S.D.

BrdU Uptake

The equivalent of 2 x 10^4 cells/100 µL (≈ 178 microcapsule/well) was placed into each well of 96-well plate. All groups were incubated with complete medium supplemented with 10% FBS for 24 h, except for the negative control group, which was incubated with starving medium supplemented with 0.1% FBS. Subsequently, 10 µM of BrdU was added to the encapsulated cells and the uptake of the thymidine analogue was allowed during an additional incubation of 24 h. Afterwards, cells were de-encapsulating with a solution of medium containing 500 µg/mL of alginate lyase (Sigma-Aldrich) and assayed for BrdU uptake employing Cell Proliferation Biotrak ELISA System (Amersham, NJ, USA) and following manufacturer's indications. Absorbances obtained for the non-specific binding control group (without BrdU) were subtracted from the rest of the groups, and results were normalized against the corresponding negative control for each time-point experiment. When assayed 2D plated cells, 2 x 10^3 cells/100 µL where seeded per well and BrdU uptake was allowed for 2h. Obtained results for 2D plated cells were extrapolated to 24h in order to be

comparable to those of the encapsulated cells. Number of cells just before adding BrdU, in the case of 2D plated cells, and number of living cells at assayed time-point, for encapsulated cells, was used to exert direct comparisons (same number of cells and same time of BrdU exposure) between them in terms proliferation rate. Data are shown as mean of 5 independent samples + S.D per study group.

Animal experimentation

For *in vivo* studies 26 adult female Balb/c mice were used as allogenic murine models. Animal studies were carried out according to the ethical guidelines established by our Institutions, under an approved animal protocol. Mice were anesthetized by isoflurane inhalation, and implanted subcutaneously with a total volume of 100 μL of cell-loaded microcapsules (suspended in additional 200 μL of PBS) using a 20-gauge catheter (Nipro; Nissho Corp, Belgium). After the first 15 days post-implantation, treated mice were injected daily for 10 days with 75 mg/kg GCV in saline solution by intraperitoneal injection. Blood samples were collected in 1.5 mL tubes (with 10 μL of 1% EDTA solution) by facial vein puncture at each time-point to measure hematrocrit. Hematocrit levels were determined after centrifugation at 3000 rpm for 15 min of whole blood using a standard microhematocrit method. Results are expressed as mean ±S.D. Once the experiment reached its goal, mice were sacrificed and samples were collected and fixed in formalin for further histology and immunohistochemistry analysis.

Detection of luciferase activity

Viability of TGL-containing enclosed cells was monitored in vivo by means of luciferase-mediated light emission. Before and after GCV treatment, mice under anesthesia (intraperitoneal administration of ketamine and xylazine mixture) were intraperitoneally administered with 3 mg of D-Luciferin in 100 μL saline (Promega, Madison, WI). After 5 min, photon emission was measured in a Xenogen IVIS 100 series luminometer living image system (Caliper Life Sciences, Hopkinton, MA). Resulted images were analyzed to quantify the luminescent signal with the Igor-Pro 2.20 software (Caliper Life Sciences).

Luciferase immunohistochemistry

Tissues were fixed in 10 % formalin, embedded in paraffin, and sectioned (5 μm in thickness). For immunohistochemistry, slides were deparaffinized and hydrated trough graded alcohols. Antigen retrieval was carried out by heating slides for 30 min at 95 ºC in Tris-EDTA (10mM Tris Base, 1mM EDTA) at pH 9. Incubation for 12 min with 3 % H_2O_2 aqueous solution was done to quench the endogenous peroxidase activity. Tissues were then incubated overnight at 4ºC with primary antibody anti-Luciferase (Europa Bioproducts) at 1:500 dilution in Dako Real antibody diluent (Dako). All slides were then incubated for 30 min at RT with Envision anti-rabbit system (Dako). Peroxidase activity was carried out with DAB (3,3'-diaminobenzidine, Dako). Finally, slides were counterstained with haematoxylin, dehydrated and mounted with DPX. One randomly taken slide per mouse was used to count the number of positively stained cell clusters

per capsule, and the results were normalized against the total number of counted capsules per slide.

Data analysis and statistics

Data are presented as mean ±S.D for line graphs and mean +S.D for bar graphs. All statistical computations were performed using IBM SPSS Statistics 19 (SPSS, Inc., Chicago, IL). Student's t-test was used to detect significant differences between two groups. One-way ANOVA was used in multiple comparisons. The Bonferroni, or Tamhane post-hoc test was applied according to the result of the Levene test of homogeneity of variances.

RESULTS

Differences in the sensitivity to GCV between encapsulated cells and cells plated onto 2D plates

First of all, we evaluated increasing concentrations of GCV on both non-encapsulated and encapsulated cells to test whether TGL transduced cells retained the same GCV sensitivity after encapsulation. As demonstrated by cell metabolic assay, encapsulated cells showed 100-fold lower sensitivity than cells plated onto 2D surfaces after 7 days of GCV treatment (Fig. 1A, B). GCV concentration of 39 nM was enough to produce a statistically significant ($p<0.001$) effect on TGL-EPO cells seeded onto flat surfaces when compared to their EPO control group (without TGL gene), whereas 3.9 µM GCV had to be used to obtain the same effect on TGL-EPO encapsulated cells. These results suggested differences in cell proliferation rates in both experimental conditions as a possible cause for these two different responses. Thus, 2D plated cells and encapsulated cells were assayed in parallel to compare their DNA synthesis rate. As expected, non-encapsulated cells proliferated much more rapidly than encapsulated cells, as revealed by their 4.7-fold higher BrdU uptake (Fig. 1C).

GCV-mediated inactivation process in vitro

Taking into account our previous results, we selected the dose of 3.9 µM to further characterize the inactivation process mediated by GCV in enclosed cells transduced with the TGL triple-fusion reporter gene. First, in a preliminary study, myoblasts plated onto flat surfaces in vitro showed a peak of caspase-3 activation at 48h after GCV

addition (Suppl. Fig. 3). Fig. 2A shows the experimental procedure carried out for encapsulated cells. The GCV untreated group showed 35 ± 2 living cells (green dots in de upper part of the dot plot) per capsule in TGL-EPO group, while 7 day GCV treatment reduced the number of living cells to 13 ± 1 ($p<0.01$) and 14 day treatment to 5 ± 1 ($p<0.01$ with respect to 7 days treatment) (Fig. 2B). Contrariwise, no differences were obtained in the EPO group, even after 14 days of treatment (Fig. 2C). Fluorescence micrographs, taken in parallel to flow cytometry assays, provide further evidence of our observations. As shown in Fig. 2B, C, images reflect the quantitative data obtained by FACS for each GCV exposure.

EPO secretion and cell proliferation after GCV treatment in vitro

Next step was to characterize how GCV-mediated inactivation process affected cell behavior and functionality within the microcapsule. Experiment design is represented in Fig. 3A. EPO secretion progressively decayed in the TGL-EPO group overtime, being the normalized EPO secretion values of 67.95%, 44.85%, 29.95% and 12.21% (for treatments of 1, 3, 7 and 14 days in that order) with respect to the GCV untreated control (Fig. 3B). In contrast, the EPO group maintained secretion levels close to 100%, regardless of GCV presence. Strikingly, statistical significant differences were achieved between the two groups after only 1 day treatment ($p<0.05$). These differences became progressively more significant overtime after GCV exposure. These results come along with those obtained for the total number of living cells per capsule.

The EPO group sustained quite similar rates of BrdU uptake, whereas DNA synthesis in the TGL-EPO group was reduced to 48.36% after 7 days of GCV treatment, and

reached 13.58% by day 14 (Fig. 3C). This value resulted near to the 9.42% expressed by the negative control. Differences between EPO and TGL-EPO groups were found statistically significant for both 7 and 14 days treatment durations ($p<0.001$).

The TGL-based biosafety system was challenged with an overdose model where a hypothetic "worst scenario" case was simulated. For this, a total cell load of 20 x 10^6 cells/mL was encapsulated varying the optimal conditions of the encapsulation process to produce defective and overloaded microcapsules that secreted large amounts of EPO (Fig. 3D). As demonstrated by quantification of EPO secretion, the exaggerated values presented by the untreated control were reduced by 97.6% after addition of GCV for 7 days ($p<0.001$).

Impact of GCV treatment on the therapeutic effects in vivo

After in vitro characterization, the effectiveness of the TGL triple-fusion reporter gene as biosafety strategy was assessed in vivo. Balb/c strain was used as allogenic recipient and a total dose of 100 µL of cells-laden microcapsules was inoculated per mouse. Three groups were formed as follows: A group of myoblasts genetically engineered to secrete EPO and express TGL was administered to 16 mice (TGL-EPO group). A second group of 5 mice was implanted with EPO-secreting but not TGL-expressing myoblasts (EPO group). TGL- expressing but not EPO-secreting cells were used for the third group of 5 mice (TGL group). As expected, 2 weeks after capsule administration, hemotocrit levels rose to 80% for EPO and TGL-EPO groups, while it was maintained around basal levels (54.8%) for the TGL group (Fig. 4A). By day 15, the TGL-EPO group showed significant differences compared to the TGL group ($p<0.001$). Treatment

(starting at day 15) with a daily dose of GCV (75 mg/kg) was administered for 10 days to TGL-EPO and EPO groups, while TGL group was left untreated. By day 57 after capsule administration (33 days after treatment), hematocrit levels of TGL-EPO group (65.7%) were comparable to those found in the TGL group (57.6%), but different ($p<0.05$) to those of the EPO group (82.7%). These differences between TGL-EPO and EPO groups became more evident by day 72 post-administration (47 days after treatment) ($p<0.01$). At this time point, hematocrit levels of TGL and TGL-EPO groups were found similar (58.4% and 61.2% respectively).

As for the luminometric assays, since only the groups carrying the TGL triple-fusion reporter gene could be eligible for the assay, the TGL-EPO group was considered as the GCV-treated group here and was compared with the TGL group, which was not subjected to GCV treatment and, thereby, considered as the untreated group. After 3 days of GCV treatment the number of detected photons diminished to 52.2% for treated mice, decreasing up to 4% at the end of the treatment (Fig. 4B). On the contrary, untreated mice sustained the initially detected photon values. Representative images of treated and untreated mice were taken before and after GCV treatment (Fig. 4C). At both time points, a strong signal was observed in encapsulated cells without treatment (untreated), whereas the light was switched off in those mice administered with the guanidine analogue (Fig. 4C).

GCV effect on the percentage of active microcapsules in vivo

In order to examine more thoroughly the GCV-mediated inactivation, immunohistochemistry was performed to detect the existence of possible remaining

active microcapsules (particles with living cells inside). As explained above, TGL-EPO group was used as the GCV-treated group and TGL group as the untreated one. Most of the microcapsule containing plugs retrieved from GCV-treated mice showed lack (or few) of microcapsules with cells stained with anti-luciferase antibody (expressed only in living cells) (Fig. 5A). On the contrary, cell clusters clearly expressing luciferase were found in all the samples from untreated mice (Fig. 5B). Quantitatively, the percentage of was 4-fold reduced due to GCV action in treated mice when compared with the untreated controls ($p<0.05$) (Fig. 5C).

DISCUSSION

Cell microencapsulation is meant to protect non-autologous cells from the immune response of the host, but more importantly, to prevent the host from undesirable effects that those foreign cells may cause. Thus, biosafety of these biosystems becomes a mandatory concern for all scientists in the field towards which efforts must be directed. In this regard, the main objective of the present work has been to test the "suicide properties" of the TGL triple-fusion reporter gene (by means of its HSV-TK fused gene), as a first step in the development of a suitable biosafety strategy to be implemented in the field of cell microencapsulation.

Previous studies using HSV-TK gene as a safety tool in cell encapsulation using GCV were carried out with cells plated onto 2D surfaces, but not with encapsulated cells [36]. However, during the last years much attention has been paid to the remarkable differences found between cell behavior of cells cultured onto 2D plates and cells embedded within a more natural 3D environment [30]. Since the GCV mechanism of action in cells bearing the HSV-TK gene is well described for cells plated onto 2D

surfaces [28], we first examined the changes that may arise as a consequence of entrapping the cells within 3D polymeric matrices. We observed that 2D plated cells were sensitive to GCV concentrations in a comparable way than that described by others (≈39 nM) (Fig. 1A) [36]. Strikingly, 100-fold higher concentration of GCV was required to induce apoptosis in encapsulated cells (Fig. 1B). As the cut-off of APA microcapsules ranges around 70 KDa [37] and GCV is a 255.2 kDa molecule, diffusion limitations does not seem feasible. Taking into account that GCV-mediated inactivation is mainly due to cell replication [28], we point out to the almost 5-fold reduced cell proliferation rate of enclosed cells (when compared to 2D plated cells) (Fig. 1C) as the most probable factor which causes this phenomenon. Indeed, cell proliferation is strongly hampered within the microcapsule due to the physical impediment exerted by the alginate matrix and the lack of cell-biomaterial interactions through focal adhesions, among others [38].

The time intervals required to achieve a notorious inactivation of entrapped cells are also increased. The 48h after GCV addition needed by 2D plated myoblasts (Suppl. Fig. 1) come along with other previously reported results in the literature for other cell lines [28]. 2D plated cells entered the apoptotic pathway uniformly, almost at the same time, unlike encapsulated cells, which needed 14 days to reach an 85% of cell death (Fig. 2). This may be due to the non-synchronized proliferation rate of encapsulated cells described by Hortelano's group [39]. EPO secretion levels correlated with viability assays and, additionally, suggest a possible inactivation effect at transcription level. This is because EPO secretion was reduced from the first day of treatment (Fig. 3B), even when GCV-mediated apoptosis has been reported to need 2 cycles post-exposure to be triggered. Importantly, BrdU uptake assays point to the hypothesis that observed

resistance in the 15% of remaining living cells after GCV treatment could be the result of a possible exit of cell cycle to G_0 (differentiation and/or quiescence), as BrdU uptake is almost undetectable after 14 days of GCV treatment (Fig. 3C).

In order to ensure that this biosafety strategy can be valid in case of adversity and uncontrolled situation, we simulated a “worst scenario" model where EPO secretion levels would be exaggeratedly increased and the overgrowth of cells might break up the semipermeable membrane, exiting the capsule to the surrounding tissue (Fig. 3D). Nonetheless, even in this severe situation, a GCV treatment of 7 days successfully mitigated the effects of EPO over-secretion, demonstrating its high grade of efficacy and reliability (Fig. 3D).

The next step was to prove the efficacy of TGL triple-fusion reporter gene in vivo, with two main objectives. On the one hand, the therapeutic effects of EPO-secreting cells had to be inhibited in mice. On the other hand, another critical point to be tested was the capacity to inactivate the implant by causing cell death in encapsulated cells, so that no risk of implant re-activation could remain. As for the first concern, we observed that ten days of GCV treatment was enough to reduce hematocrit levels of TGL-expressing and EPO-secreting cells close to those of the control group (only TGL-expressing cells) 33 days after finishing the treatment. Moreover, 47 days after the last GCV administration, levels in both groups were practically undistinguishable (Fig. 4A). This delay may be justified by the fact that the estimated lifespan of erythrocytes in mice is between 41 and 52 days [40]. In this regard, the TGL triple-fusion reporter gene may be of a great interest, since we were able to monitor the decay of emitted photons, and thereby cell viability, in TGL-bearing and GCV-treated cells in vivo (Fig. 4B, C). We observed that

after 3 days of treatment, the viability of encapsulated cells was reduced to half. On the contrary, GCV treatment had no effect on the non TGL-expressing but EPO-secreting cells, which maintained hematocrit levels of 80.3%, thus proving the lack of toxicity, at least, for assayed concentration (75 mg/Kg). This is of remarkable importance because we found that, according to the literature [41], higher doses of GCV (150mg/Kg) resulted toxic and caused death in treated mice (data not shown).

Regarding the second point, we sought the GCV effects at cellular level to confirm that the treatment with GCV left no remaining living cells. Immunohistochemistry performed in retrieved microcapsules revealed that the number of cell clusters positively stained with an anti-luciferase antibody, and hence living cells, was dramatically decreased in treated mice when compared with untreated ones (Fig. 5). However, results showed few but still remaining active cells within the microcapsules of treated mice. This is in keeping with the results obtained in vitro, where a small percentage of encapsulated cells resistant to GCV treatment could be observed. Among the possible explanations for this fact, it seems reasonable that the same proliferation arrest found in vitro might occur in vivo, hindering the apoptotic response.

Thus, even if this strategy seems to be unable to inactivate the 100% of the implant, remaining cells stay in a non-proliferative state, which reduces considerably the risk of host tissue invasion by encapsulated cells. Moreover, in case of deleterious effects, the action of GCV is visible from the first day of treatment, in which the secretion of the therapeutic factor is reduced to half (Fig. 3B). In addition, in the hypothetic case that cells can break the capsule and/or come out to start dividing, this proliferation would make them more vulnerable to GCV effects. Besides, encapsulated cells tend to form

aggregates due to the physical constraints exerted by the alginate matrix, which maintains the cells in a close contact with each other (Fig. 5). This fact would favor the intercellular intoxication given through gap junctions known as “bystander killing” effect [28], and would reinforce the safety of this biosystem.

Future studies should be focused on regulating EPO expression by different means, while designing new tools that use other drugs instead of GCV. Simultaneously, additional efforts should be directed towards the development of new strategies where induction of apoptosis can be decoupled from cell replication, so that greater control over implant inactivation may be achieved. Likely, the use of this kind of suicide genes may be also applicable in a near future to those drug delivery or cell delivery approaches using engineered cells derived from different sources, such as immortalized mesenchymal stem cells (MSCs) or induced pluripotent stem cells (IPSs) for example. In fact, even some approaches employing primary MSCs are increasingly demanding biosafety tools to incorporate into the genome of their cells [42].

CONCLUSION

The present work provides meaningful insight regarding GCV-mediated inactivation in encapsulated cells bearing TGL triple-fusion reporter gene through its fused HSV-TK suicide gene. Here, it has been proved that GCV causes a dramatic decrease in the number of living cells per capsule, drastic reduction of EPO secretion and cell proliferation arrest, giving rise to a disappearance of the therapeutic effects and restoration of the hematocrit levels in mice implanted with encapsulated cells carrying TGL triple-fusion reporter gene and engineered to secrete EPO. We conclude that the

inclusion of inactivation gene vectors in the genome of encapsulated cells may represent a valuable strategy to overcome some of the biosafety concerns in the field of cell microencapsulation. In this study, TGL triple-fusion reporter gene demonstrated satisfactory results in regulating the release of therapeutic factors, and it is proposed as a starting point to work in this direction.

ACKNOWLEDGMENTS

Authors would like to thank Raúl Catena for cell transduction and his invaluable advice. We also thank Miriam Redrado for technical help with immunochemistry for luciferase.

IN MEMORIAM

In memoriam of Dr Ainhoa Murua, who not only blessed us with her kindness, but she also provided us with the willingness and enthusiasm needed to embark on this journey. You will always be an example to be followed and our inspiration in the search of knowledge.

REFERENCES

1. Hernández RM, Orive G, Murua A, Pedraz JL. Microcapsules and microcarriers for in situ cell delivery. Adv Drug Deliv Rev 2010;62:711-730.

2. Calafiore R, Basta G, Luca G, Lemmi A, Montanucci MP, Calabrese G, et al. Microencapsulated pancreatic islet allografts into nonimmunosuppressed patients with type 1 diabetes: first two cases. Diabetes Care 2006;29:137-138.

3. Sieving PA, Caruso RC, Tao W, Coleman HR, Thompson DJ, Fullmer KR, et al. Ciliary neurotrophic factor (CNTF) for human retinal degeneration: phase I trial of CNTF delivered by encapsulated cell intraocular implants. Proc Natl Acad Sci U S A 2006;103:3896-3901.

4. Bloch J, Bachoud-Levi AC, Deglon N, Lefaucheur JP, Winkel L, Palfi S, et al. Neuroprotective gene therapy for Huntington's disease, using polymer-encapsulated cells engineered to secrete human ciliary neurotrophic factor: results of a phase I study. Hum Gene Ther 2004;15:968-975.

5. Salmons B, Lohr M, Gunzburg WH. Treatment of inoperable pancreatic carcinoma using a cell-based local chemotherapy: results of a phase I/II clinical trial. J Gastroenterol 2003;38 Suppl 15:78-84.

6. Lohr M, Hoffmeyer A, Kroger J, Freund M, Hain J, Holle A, et al. Microencapsulated cell-mediated treatment of inoperable pancreatic carcinoma. Lancet 2001;357:1591-1592.

7. Aebischer P, Schluep M, Deglon N, Joseph JM, Hirt L, Heyd B, et al. Intrathecal delivery of CNTF using encapsulated genetically modified xenogeneic cells in amyotrophic lateral sclerosis patients. Nat Med 1996;2:696-699.

8. Goren A, Dahan N, Goren E, Baruch L, Machluf M. Encapsulated human mesenchymal stem cells: a unique hypoimmunogenic platform for long-term cellular therapy. FASEB J 2010;24:22-31.

9. Gautier A, Carpentier B, Dufresne M, Vu Dinh Q, Paullier P, Legallais C. Impact of alginate type and bead diameter on mass transfers and the metabolic activities of encapsulated C3A cells in bioartificial liver applications. Eur Cell Mater 2011;21:94-106.

10. Veriter S, Aouassar N, Adnet PY, Paridaens MS, Stuckman C, Jordan B, et al. The impact of hyperglycemia and the presence of encapsulated islets on oxygenation within a bioartificial pancreas in the presence of mesenchymal stem cells in a diabetic Wistar rat model. Biomaterials 2011;32:5945-5956.

11. de Vos P, Bucko M, Gemeiner P, Navratil M, Svitel J, Faas M, et al. Multiscale requirements for bioencapsulation in medicine and biotechnology. Biomaterials 2009;30:2559-2570.

12. Kim K, Liu X, Zhang Y, Cheng J, Yu Wu X, Sun Y. Elastic and viscoelastic characterization of microcapsules for drug delivery using a force-feedback MEMS microgripper. Biomed Microdevices 2009;11:421-427.

13. Leung A, Trau M, Nielsen LK. Assembly of multilayer PSS/PAH membrane on coherent alginate/PLO microcapsule for long-term graft transplantation. J Biomed Mater Res A 2009;88:226-237.

14. Williams DF. On the mechanisms of biocompatibility. Biomaterials 2008;29:2941-2953.

15. Tam SK, Dusseault J, Bilodeau S, Langlois G, Halle JP, Yahia L. Factors influencing alginate gel biocompatibility. J Biomed Mater Res A 2011;98:40-52.

16. Tam SK, Bilodeau S, Dusseault J, Langlois G, Halle JP, Yahia LH. Biocompatibility and physicochemical characteristics of alginate-polycation microcapsules. Acta Biomater 2011;7:1683-1692.

17. Baruch L, Benny O, Gilert A, Ukobnik M, Ben Itzhak O, Machluf M. Alginate-PLL cell encapsulation system co-entrapping PLGA-microspheres for the continuous release of anti-inflammatory drugs. Biomed Microdevices 2009;11:1103-1113.

18. Orive G, De Castro M, Kong HJ, Hernandez RM, Ponce S, Mooney DJ, et al. Bioactive cell-hydrogel microcapsules for cell-based drug delivery. J Control Release 2009;135:203-210.

19. Santos E, Orive G, Calvo A, Catena R, Fernández-Robredo P, Layana AG, et al. Optimization of 100 μm alginate-poly-l-lysine-alginate capsules for intravitreous administration. J Controlled Release 2012;158:443-450.

20. Sakai S, Hashimoto I, Tanaka S, Salmons B, Kawakami K. Small agarose microcapsules with cell-enclosing hollow core for cell therapy: transplantation of ifosfamide-activating cells to the mice with preestablished subcutaneous tumor. Cell Transplant 2009;18:933-939.

21. Murua A, Orive G, Hernandez RM, Pedraz JL. Xenogeneic transplantation of erythropoietin-secreting cells immobilized in microcapsules using transient immunosuppression. J Control Release 2009;137:174-178.

22. Sgroi A, Mai G, Morel P, Baertschiger RM, Gonelle-Gispert C, Serre-Beinier V, et al. Transplantation of encapsulated hepatocytes during acute liver failure improves survival without stimulating native liver regeneration. Cell Transplant 2011;20:1791–1803.

23. Zhang H, Zhu SJ, Wang W, Wei YJ, Hu SS. Transplantation of microencapsulated genetically modified xenogeneic cells augments angiogenesis and improves heart function. Gene Ther 2008;15:40-48.

24. Vaithilingam V, Quayum N, Joglekar MV, Jensen J, Hardikar AA, Oberholzer J, et al. Effect of alginate encapsulation on the cellular transcriptome of human islets. Biomaterials 2011;32:8416-8425.

25. Montanucci P, Pennoni I, Pescara T, Blasi P, Bistoni G, Basta G, et al. The functional performance of microencapsulated human pancreatic islet-derived precursor cells. Biomaterials 2011;32:9254-9262.

26. Catena R, Santos E, Orive G, Hernández RM, Pedraz JL, Calvo A. Improvement of the monitoring and biosafety of encapsulated cells using the SFGNESTGL triple reporter system. J Controlled Release 2010;146:93-98.

27. Deglon N, Heyd B, Tan SA, Joseph JM, Zurn AD, Aebischer P. Central nervous system delivery of recombinant ciliary neurotrophic factor by polymer encapsulated differentiated C2C12 myoblasts. Hum Gene Ther 1996;7:2135-2146.

28. Tomicic MT, Thust R, Kaina B. Ganciclovir-induced apoptosis in HSV-1 thymidine kinase expressing cells: critical role of DNA breaks, Bcl-2 decline and caspase-9 activation. Oncogene 2002;21:2141-2153.

29. Mullen CA. Metabolic suicide genes in gene therapy. Pharmacol Ther 1994;63:199-207.

30. Santos E, Hernandez RM, Pedraz JL, Orive G. Novel advances in the design of three-dimensional bio-scaffolds to control cell fate: translation from 2D to 3D. Trends Biotechnol 2012;30:331-341.

31. Chateauvieux S, Grigorakaki C, Morceau F, Dicato M, Diederich M. Erythropoietin, erythropoiesis and beyond. Biochem Pharmacol 2011;82:1291-1303.

32. Zhu J, Emerson SG. Hematopoietic cytokines, transcription factors and lineage commitment. Oncogene 2002;21:3295-3313.

33. Kariko K, Muramatsu H, Keller JM, Weissman D. Increased erythropoiesis in mice injected with submicrogram quantities of pseudouridine-containing mRNA encoding erythropoietin. Mol Ther 2012;20:948-953.

34. Ponomarev V, Doubrovin M, Serganova I, Vider J, Shavrin A, Beresten T, et al. A novel triple-modality reporter gene for whole-body fluorescent, bioluminescent, and nuclear noninvasive imaging. Eur J Nucl Med Mol Imaging 2004;31:740-751.

35. Lim F, Sun A. Microencapsulated islets as bioartificial endocrine pancreas. Science 1980;210:908-910.

36. Aebischer P, Pochon NA, Heyd B, Deglon N, Joseph JM, Zurn AD, et al. Gene therapy for amyotrophic lateral sclerosis (ALS) using a polymer encapsulated xenogenic cell line engineered to secrete hCNTF. Hum Gene Ther 1996;7:851-860.

37. Leung A, Nielsen LK, Trau M, Timmins NE. Tissue transplantation by stealth—coherent alginate microcapsules for immunoisolation. Biochem Eng J 2010;48:337-347.

38. Hill E, Boontheekul T, Mooney DJ. Designing scaffolds to enhance transplanted myoblast survival and migration. Tissue Eng 2006;12:1295-1304.

39. Thakur A, Sengupta R, Matsui H, Lillicrap D, Jones K, Hortelano G. Characterization of viability and proliferation of alginate-poly-L-lysine-alginate encapsulated myoblasts using flow cytometry. J Biomed Mater Res B Appl Biomater 2010;94:296-304.

40. Provencher Bolliger A, Everds EN, Zimmerman LK, Moore MD, Smith AS, Barnhart FK. Hematology of laboratory animals. In: Weiss D, Wardrop KJ, editors. Schalm´s Veterinary Hematology (Sixth Edition): John Wiley & Sons Inc, 2010. p. 852-887.

41. Duan J, Paris W, Kibler P, Bousquet C, Liuzzi M, Cordingley MG. Dose and duration-dependence of ganciclovir treatment against murine cytomegalovirus infection in severe combined immunodeficient mice. Antiviral Res 1998;39:189-197.

42. Kauer TM, Figueiredo JL, Hingtgen S, Shah K. Encapsulated therapeutic stem cells implanted in the tumor resection cavity induce cell death in gliomas. Nat Neurosci 2011;15:197-204.

FIGURE LEGENDS

Figure 1. GCV sensitivity for cells plated onto 2D surfaces (A) and encapsulated cells (B). In both cases, the TGL-EPO group and the EPO group were subjected to increasing concentrations of GCV during 7 days. (C) BrdU uptake, assessed with equal number of 2D plated cells and encapsulated cells. Y axis represents the fold increase of BrdU acquisition with regard to the negative control (cells seeded with 0.1% FBS supplemented medium). Line graphs are built with the mean values ±S.D (n=7). Bar graph represents the mean +S.D (n=5). Statistical significance *p<0.05 and ***p<0.001.

Figure 2. (A) Experimental design to assess the number of living cells per capsule in GCV-mediated inactivation process at different time points. Flow cytometry data, together with fluorescence micrographs depicting the effects of GCV in the TGL-EPO group (B) and in the EPO group (C) after 7 and 14 days of treatment. Green dots in the upper part of calcein/ethidium homodimer-1 dot plots represent the population of living cells. Bar graphs symbolize the mean +S.D (n=3). Statistical significance **p<0.01. Scale bars = 100 µm.

Figure 3. (A) Experimental design to assess EPO secretion (B) and BrdU uptake (C) during GCV-mediated inactivation process at different time points. Both EPO secretion levels (B) and BrdU uptake (C) obtained from untreated control group were considered as 100% in each group and all values were expressed in function of this percentage. (D) Micrographs of the hypothetical “worst scenario” model and the impact of GCV treatment on EPO secretion levels after a 7-day treatment. Bar graphs show the mean +S.D (n=3 for EPO secretion assays; n=5 for BrdU uptake). Statistical significance *p<0.05, **p<0.01 and ***p<0.001. Scale bars = 200 µm.

Figure 4. (A) Hematocrit levels of mice implanted with different groups and the effects caused by GCV treatment. (B) Luminometry reflecting the photon emission of both treated and untreated mice before, after and during the treatment. Emitted photon flux before GCV treatment was taken as the 100%, and the photon emissions obtained during and after treatment were normalized as a percentage of the initial value for each mouse. (C) Light emission was captured before and after GCV treatment for both TGL-EPO (GCV-treated) and TGL (untreated) mice. Line graphs are depicted as the mean ±S.D (n = 16 TGL-EPO group; n = 5 EPO group; n = 5 control group). Statistical significance ###p<0.001 between TGL-EPO and TGL groups; *p<0.05 and **p<0.01 between TGL-EPO and EPO groups. Colored bar represents the GCV treatment duration.

Figure 5. (A-C) Immunohistochemistry confirmed that the percentage of active microcapsules decreases remarkably in treated mice (A) when compared with untreated mice (B) after GCV treatment. (C) The percentage of active microcapsules (Luc +) was determined on the basis of the number of microcapsules containing cell clusters positively stained with anti-luciferase antibody (expressed only in living cells) with respect to the total amount of microcapsules per slide (one slide per mouse). Scale bars in (A, B) = 300 µm; Inset magnification in (B) = 100 µm. Arrows in (B) point out the presence of cell clusters positively stained with anti-luciferase antibody. Bar graph is depicted as the mean +S.D (n = 16 TGL-EPO "GCV-treated"; n = 5 TGL "untreated"). Statistical significance *$p<0.05$.

SUPPLEMENTARY MATERIAL

Supplementary Figure 1. Flow cytometry histogram of GFP+ cells after transduction with $pSFG_{NES}TGL$ plasmid. TGL triple-fusion reporter gene-containing cells were sorted by FACS for the enrichment of the GFP+ cell population, until obtaining more than 95% of GFP^+ cells.

Supplementary Figure 2. Clone characterization for EPO secretion. All employed clones in this study were assayed for EPO secretion to verify that $pSFG_{NES}TGL$ plasmid do not cause alterations in the secretion levels of the therapeutic factor. TGL clone = Pure C_2C_{12} myoblasts transduced with $pSFG_{NES}TGL$ plasmid. EPO clone = EPO-secreting C_2C_{12} myoblasts. TGL-EPO clone = EPO-secreting C_2C_{12} myoblasts transduced with $pSFG_{NES}TGL$ plasmid. Bar graphs symbolize the mean +S.D (n=3). N.D. = Non-detected.

Supplementary Figure 3. Percentage of active caspase-3 after GCV addition in C_2C_{12}-TGL-EPO cells plated onto 2D surfaces. TGL-containing 2D plated cells were subjected to increasing GCV (3.9 μM) time exposures and the effects of the guanidine analogue in the percentage of active caspase-3 were assessed by flow cytometry together with an untreated control. Bars represent the percentage of active caspase-3 obtained for each time exposure.

Supplementary Material And Methods

Clone characterization for EPO secretion

TGL-expressing but no EPO-secreting (TGL), EPO expressing but no TGL-expressing (EPO), and TGL-expressing and EPO-secreting (TGL-EPO) cell clones were assayed for EPO secretion. 1 x 10^6 cells from each cell clone (x3) were seeded per well in a 6 well plate. After 4h of incubation, cell supernatants were taken to further analyze them by using the Quantikine IVD Human Erythropoietin ELISA Kit (R&D Systems, Minneapolis, MN). Standards and samples were run in duplicate according to the procedure specified in the kit. Results are expressed as mean + S.D.

Caspase-3 activation in 2D plated C_2C_{12} after GCV addition

1 x 10^5 cells were seeded per well in a 6 well plate. 3.9 µM of GCV was added into each well at different time points, so that increasing time exposures to GCV were obtained. All time exposures were assayed by flow cytometry together with an untreated group using PE Active Caspase-3 Apoptosis Kit (BD Pharmingen) and following manufacturer's indications. Results are shown as the percentage of active caspase-3 obtained for each time exposure and the control.

Figure 1.

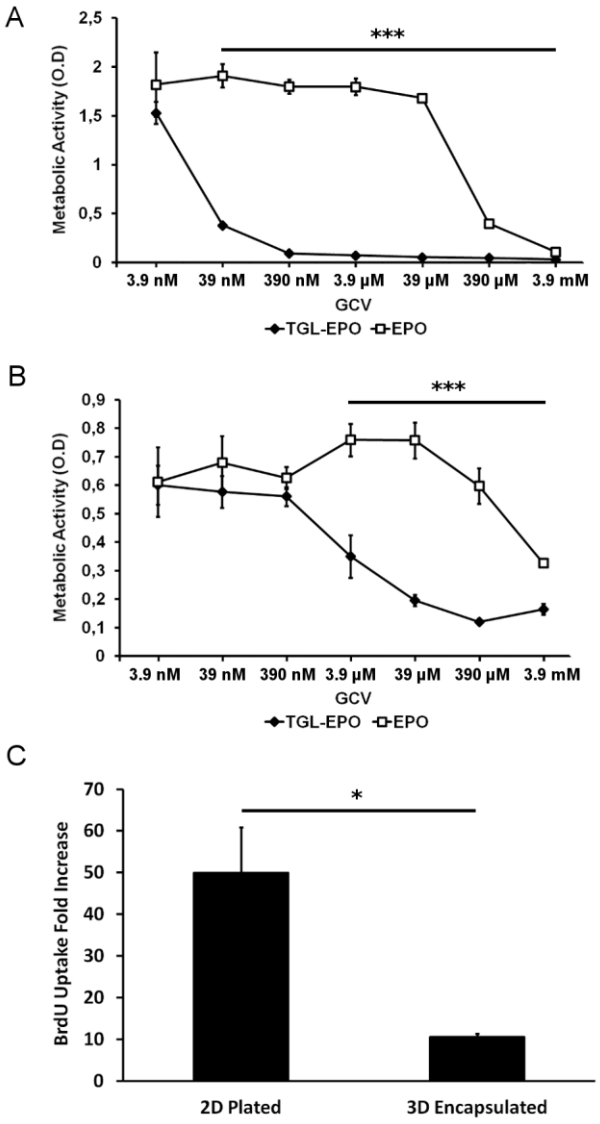
A
***
Metabolic Activity (O.D)
2,5
2
1,5
1
0,5
0
3.9 nM
39 nM
390 nM
3.9 µM
39 µM
390 µM
3.9 mM
GCV
TGL-EPO
EPO
B
***
Metabolic Activity (O.D)
0,9
0,8
0,7
0,6
0,5
0,4
0,3
0,2
0,1
0
3.9 nM
39 nM
390 nM
3.9 µM
39 µM
390 µM
3.9 mM
GCV
TGL-EPO
EPO
C
*
BrdU Uptake Fold Increase
70
60
50
40
30
20
10
0
2D Plated
3D Encapsulated

Figure 2.

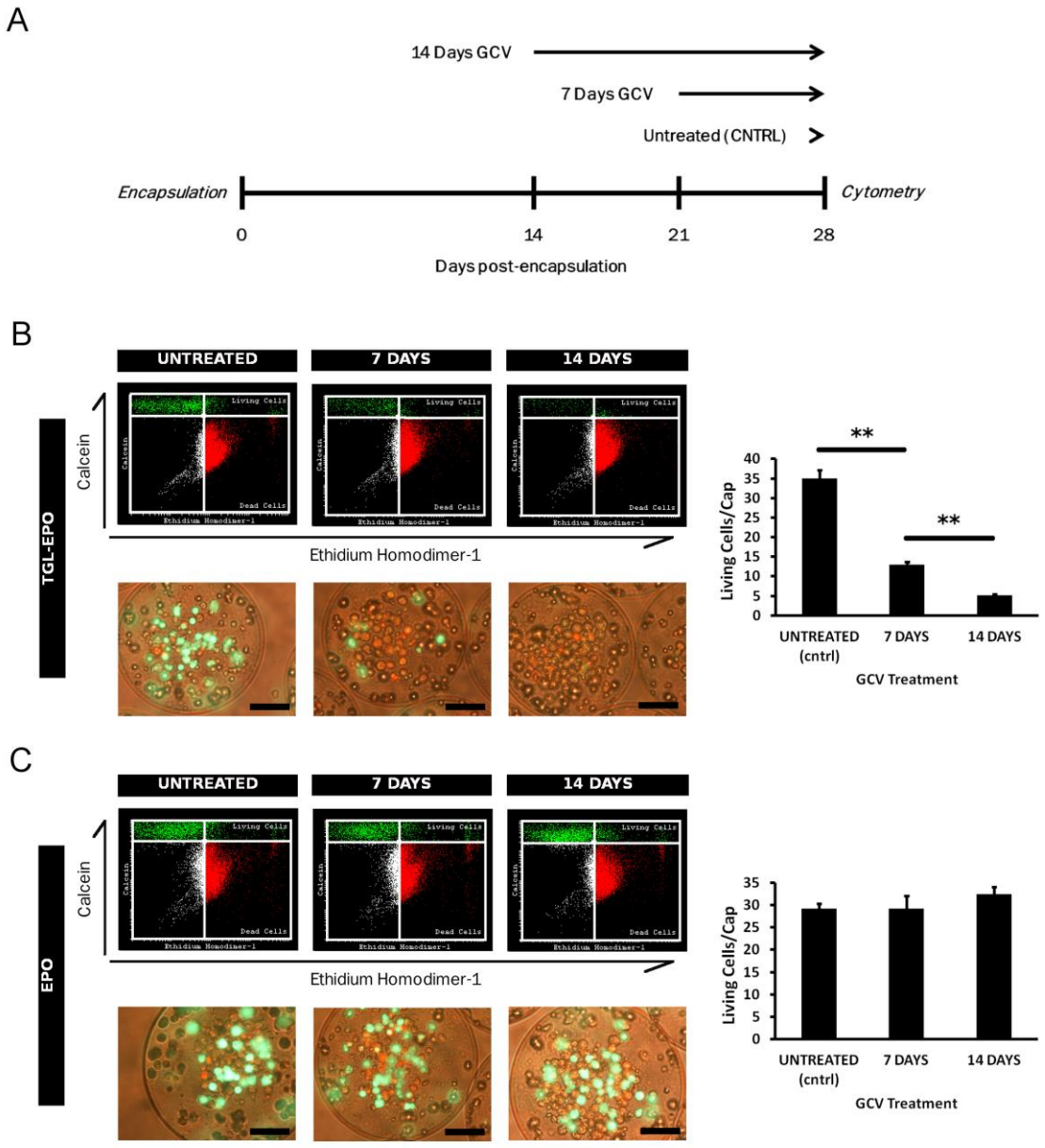
A
14 Days GCV
7 Days GCV
Untreated (CNTRL)
Encapsulation
Cytometry
0
14
21
28
Days post-encapsulation
B
UNTREATED
7 DAYS
14 DAYS
TGL-EPO
Calcein
Ethidium Homodimer-1
Living Cells
Dead Cells
Living Cells/Cap
UNTREATED (cntrl)
7 DAYS
14 DAYS
GCV Treatment
C
EPO

Figure 3.

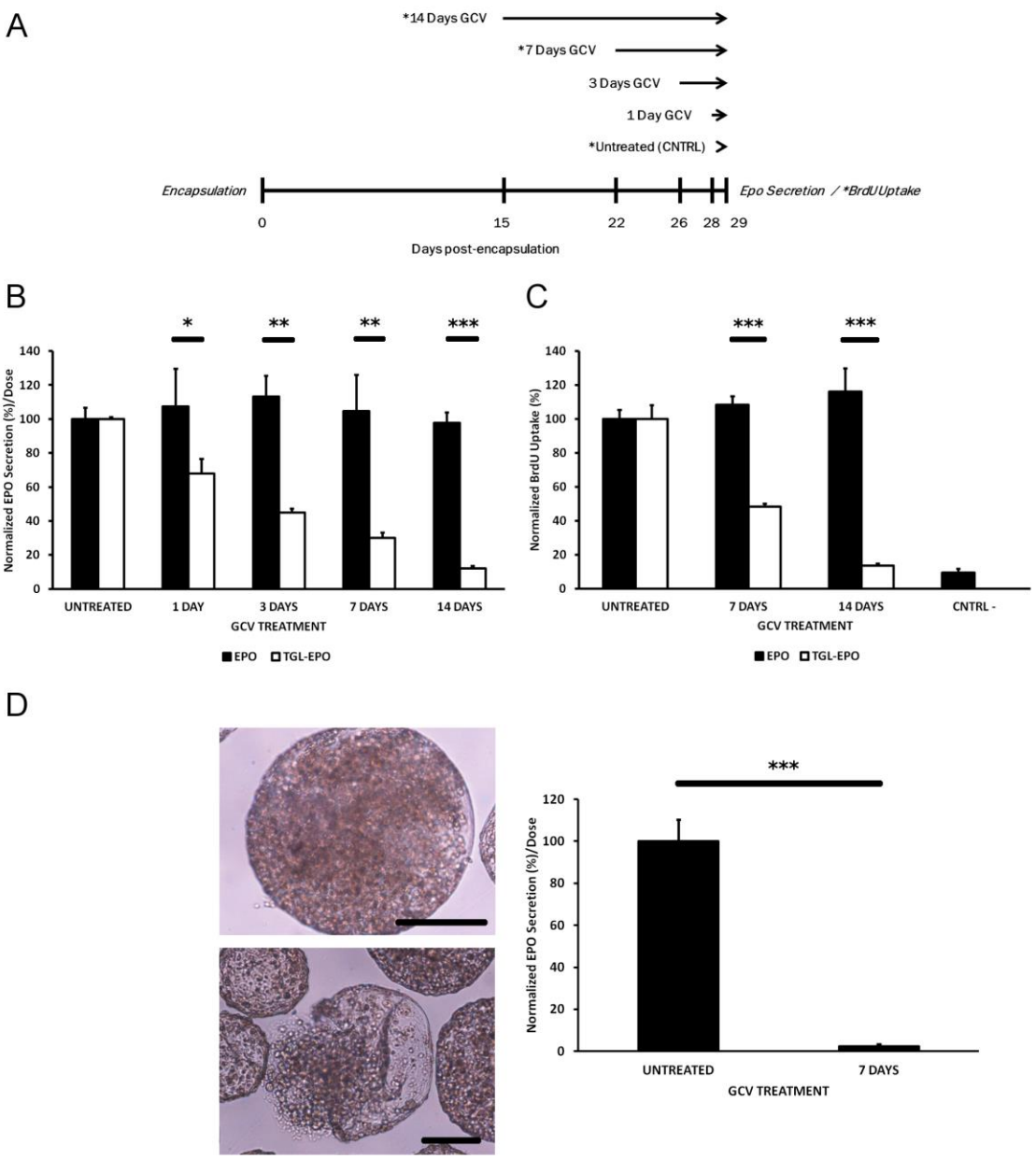
A
*14 Days GCV
*7 Days GCV
3 Days GCV
1 Day GCV
*Untreated (CNTRL)
Encapsulation
Epo Secretion / *BrdU Uptake
0
15
22
26
28
29
Days post-encapsulation
B
Normalized EPO Secretion (%)/Dose
UNTREATED
1 DAY
3 DAYS
7 DAYS
14 DAYS
GCV TREATMENT
EPO
TGL-EPO
C
Normalized BrdU Uptake (%)
UNTREATED
7 DAYS
14 DAYS
CNTRL -
GCV TREATMENT
EPO
TGL-EPO
D
Normalized EPO Secretion (%)/Dose
UNTREATED
7 DAYS
GCV TREATMENT

Figure 4.

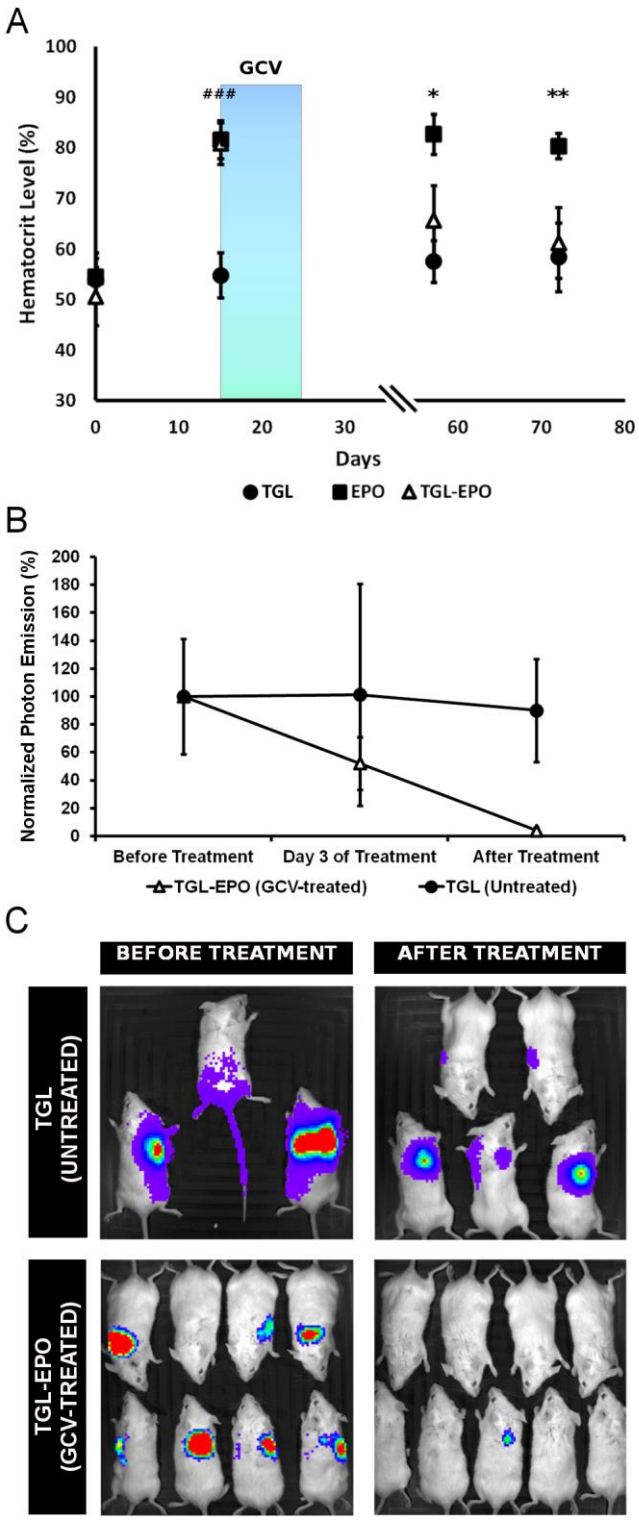
A
GCV
###
*
**
Hematocrit Level (%)
100
90
80
70
60
50
40
30
0
10
20
30
60
70
80
Days
TGL
EPO
TGL-EPO
B
Normalized Photon Emission (%)
200
180
160
140
120
100
80
60
40
20
0
Before Treatment
Day 3 of Treatment
After Treatment
TGL-EPO (GCV-treated)
TGL (Untreated)
C
BEFORE TREATMENT
AFTER TREATMENT
TGL (UNTREATED)
TGL-EPO (GCV-TREATED)

Figure 5.

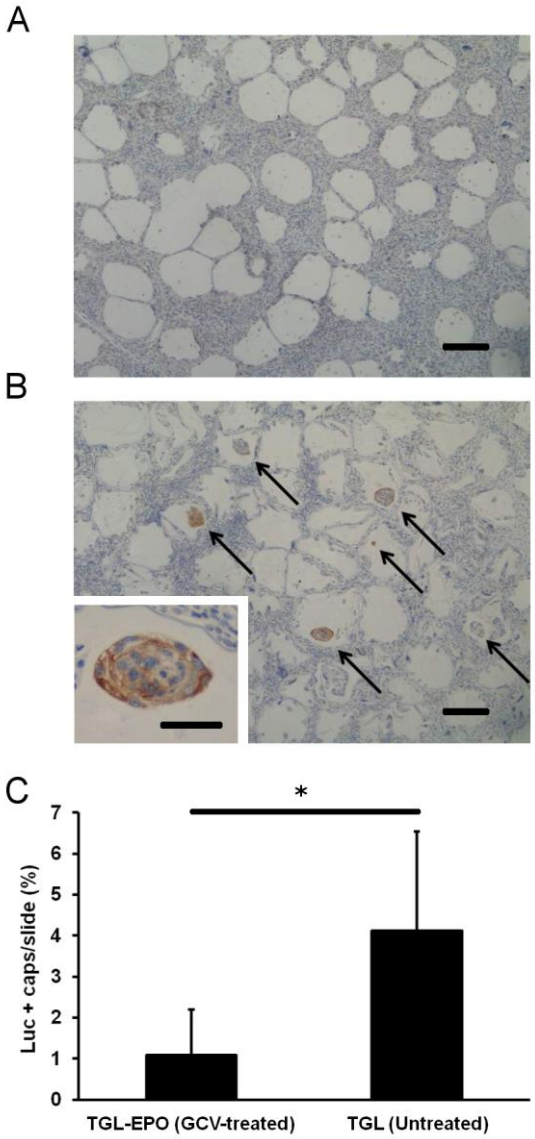
A
B
C
*
Luc + caps/slide (%)
0
1
2
3
4
5
6
7
TGL-EPO (GCV-treated)
TGL (Untreated)

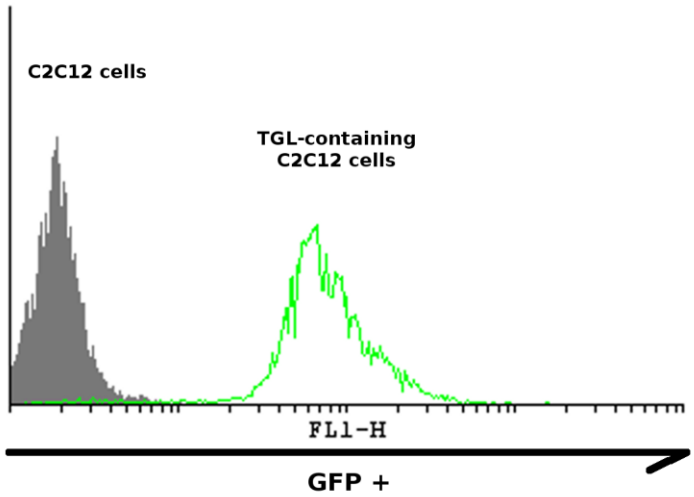

Supplementary Figure 1. Flow cytometry histogram of GFP+ cells after transduction with pSFGNESTGL plasmid. TGL triple-fusion reporter gene-containing cells were sorted by FACS for the enrichment of the GFP+ cell population, until obtaining more than 95% of GFP+ cells.

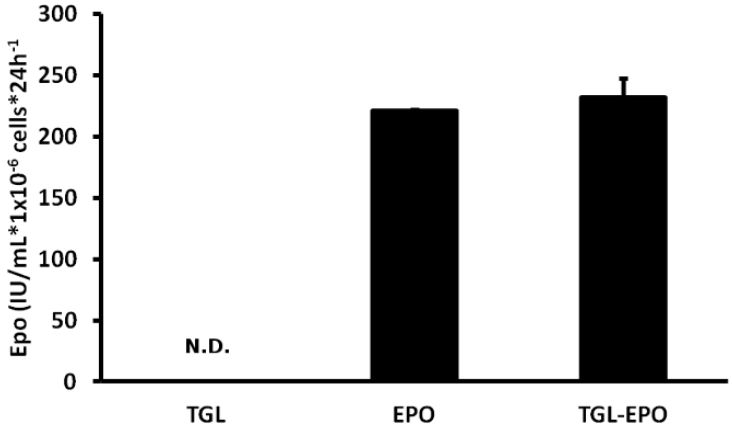

Supplementary Figure 2. Clone characterization for EPO secretion. All employed clones in this study were assayed for EPO secretion to verify that pSFGNESTGL plasmid do not cause alterations in the secretion levels of the therapeutic factor. TGL clone = Pure C2C12 myoblasts transduced with pSFGNESTGL plasmid. EPO clone = EPO-secreting C2C12 myoblasts. TGL-EPO clone = EPO-secreting C2C12 myoblasts transduced with pSFGNESTGL plasmid. Bar graphs symbolize the mean +S.D (n=3). N.D. = Non-detected.

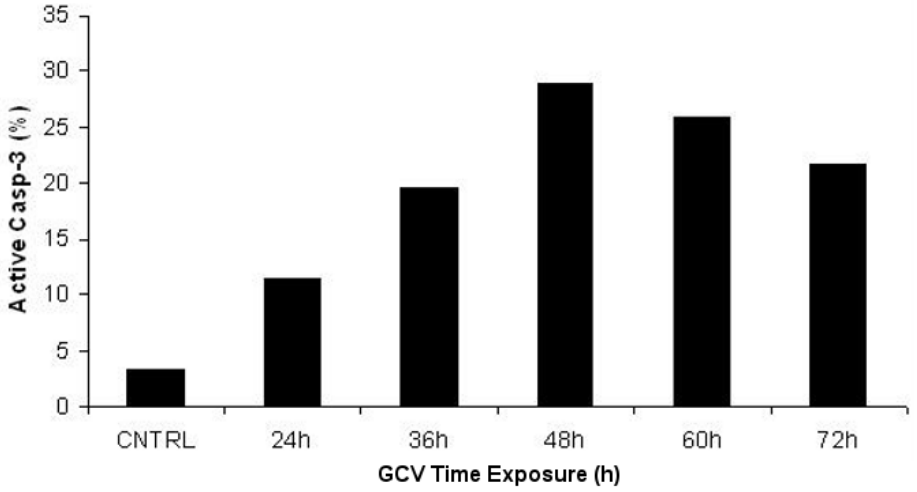

Supplementary Figure 3. Percentage of active caspase-3 after GCV addition in C2C12-TGL-EPO cells plated onto 2D surfaces. TGL-containing 2D plated cells were subjected to increasing GCV (3.9 μM) time exposures and the effects of the guanidine analogue in the percentage of active caspase-3 were assessed by flow cytometry together with an untreated control. Bars represent the percentage of active caspase-3 obtained for each time exposure.